Controlled Synthesis of Ordered Mesoporous C−TiO_2 Nanocomposites with Crystalline Titania Frameworks from Organic−Inorganic−Amphiphilic Coassembly†

Ruili Liu, Yingjie Ren, Yifeng Shi, Fan Zhang, Lijuan Zhang, Bo Tu, and Dongyuan Zhao*

Department of Chemistry and Shanghai Key Laboratory of Molecular Catalysis and Innovative Materials, Key Laboratory of Molecular Engineering of Polymers, Advanced Materials Laboratory, Fudan University, Shanghai 200433, P. R. China

Received May 31, 2007. Revised Manuscript Received July 19, 2007

Highly ordered mesoporous carbon−titania nanocomposites with nanocrystal-glass frameworks have been synthesized via the organic−inorganic−amphiphilic coassembly followed by the in situ crystallization technology. A soluble resol polymer was used as a carbon precursor, prehydrolyzed $TiCl_4$ as an inorganic precursor, and triblock copolymer F127 as a template. The carbon−titania nanocomposites with controllable texture properties and composition can be obtained in a wide range from 20 to 80 wt% TiO_2 by adjusting the initial mass ratios. The C−TiO_2 nanocomposites with "bricked-mortar"frameworks exhibit highly ordered 2D hexagonal mesostructure and high thermal stability up to 700 °C. The nanocomposites have high surface area (465 m^2 g^{-1}) and large pore size (∼4.1 nm). Additionally, the nanocomposites show good performance in degradation of Rhodamine B due to the photocatalytic activity of the titania nanocrystals and the strong adsorptive capacity of the glasslike carbon.

Introduction

Titania-based materials are of considerable interest because of their unique photoinduced electron transfer, high chemical stability, and low cost,[1,2] as well as for their great applications in photoconductors, sensors, photocatalysts, and dye-sensitized solar cells.[3–7] Increasing attention has been focused on the simultaneous achievement of high crystallinity and ordered mesoporous TiO_2 frameworks with high thermal stability.[8,9] Ordered large channels facilitate diffusion within the frameworks and thermal behavior of mesoporous titania materials is of central importance to the practical applications. It is well-known that the intrinsic properties of nanocrystalline titania are strongly dependent on the phase and crystallite size of the anatase comprising the mesopore walls. However, typically for mesoporous TiO_2, the thermal treatment employed to transform amorphous titania to crystalline pore walls usually leads to a collapse of the mesoporous frameworks.[10–12] Attempts to increase the thermal stability of mesoporous titania have intensely been explored by the special post-treatment[13–16] and formation of thick pore walls.[17,18] Despite all these efforts, the fabrication of mesoporous titania with fully crystalline frameworks is still a great challenge, mainly because of the unmatching symmetries and high distortion energy between the mesostructure and crystallized TiO_2.

An alternative method is to add amorphous components, such as phosphoxides[19] or carbon,[4] into the mesostructured TiO_2 framework, which can form a glasslike phase; it is responsible for the stability of ordered mesostructures. The glass components work as a binder to glue TiO_2 nanocrystals in the frameworks, resulting in ordered mesostructure with a nanocrystal-glass configuration. The bricked-mortar frameworks demonstrate a good combination of a large surface area and high thermal stability with a controllable microstructure of crystalline TiO_2. The mesoporous carbon−titania

† Part of the "Templated Materials Special Issue".

* To whom correspondence should be addressed. Tel: 86-21-5566-4194. Fax: 86-21-5566-4190. E-mail: dyzhao@fudan.edu.cn.

(1) Soler-illia, G. J. D.; Sanchez, C.; Lebeau, B.; Patarin, J. *Chem. Rev.* **2002**, *102*, 4093.
(2) He, X.; Antonelli, D. *Angew. Chem., Int. Ed.* **2001**, *41*, 214.
(3) Hagfeldt, A.; Gratzel, M. *Chem. Rev.* **1995**, *95*, 49.
(4) Tang, J.; Wu, Y. Y.; McFarland, E. W.; Stucky, G. D. *Chem. Commun.* **2004**, 1670.
(5) Bach, U.; Lupo, D.; Comte, P.; Moser, J. E.; Weissortel, F.; Salbeck, J.; Spreitzer, H.; Gratzel, M. *Nature* **1998**, *395*, 583.
(6) Prene, P.; Lancelle-Beltran, E.; Boscher, C.; Belleville, P.; Buvat, P.; Sanchez, C. *Adv. Mater.* **2006**, *18*, 2579.
(7) Zukalova, M.; Zukal, A.; Kavan, L.; Nazeeruddin, M. K.; Liska, P.; Gratzel, M. *Nano Lett.* **2005**, *5*, 1789.
(8) Torimoto, T.; Ito, S.; Kuwabata, S.; Yoneyama, H. *Environ. Sci. Technol.* **1996**, *30*, 1275.
(9) Sopyan, I.; Watanabe, M.; Murasawa, S.; Hashimoto, K.; Fujishima, A. *J. Electr. Chem.* **1996**, *415*, 183.
(10) Yang, P. D.; Zhao, D. Y.; Margolese, D. I.; Chmelka, B. F.; Stucky, G. D. *Nature* **1998**, *396*, 152.
(11) Yun, H. S.; Miyazawa, K.; Zhou, H. S.; Honma, I.; Kuwabara, M. *Adv. Mater.* **2001**, *13*, 1377.
(12) Schuth, F. *Chem. Mater.* **2001**, *13*, 3184.
(13) Cassiers, K.; Linssen, T.; Meynen, V.; Van der Voort, P.; Cool, P.; Vansant, E. F. *Chem. Commun.* **2003**, 1178.
(14) Wang, K. X.; Morris, M. A.; Holmes, J. D. *Chem. Mater.* **2005**, *17*, 1269.
(15) Grosso, D.; Soler-Illia, G.; Crepaldi, E. L.; Cagnol, F.; Sinturel, C.; Bourgeois, A.; Brunet-Bruneau, A.; Amenitsch, H.; Albouy, P. A.; Sanchez, C. *Chem. Mater.* **2003**, *15*, 4562.
(16) Choi, H.; Sofranko, A. C.; Dionysiou, D. D. *Adv. Funct. Mater.* **2006**, *16*, 1067.
(17) Choi, S. Y.; Mamak, M.; Coombs, N.; Chopra, N.; Ozin, G. A. *Adv. Funct. Mater.* **2004**, *14*, 335.
(18) Smarsly, B.; Grosso, D.; Brezesinski, T.; Pinna, N.; Boissiere, C.; Antonietti, M.; Sanchez, C. *Chem. Mater.* **2004**, *16*, 2948.
(19) Li, D. L.; Zhou, H. S.; Honma, I. *Nat. Mater.* **2004**, *3*, 65.

10.1021/cm071470w CCC: $40.75
Published on Web 09/26/2007

nanocomposites may have the advantages of coupling the photoactivity of anatase-type TiO_2 with the adsorptive capacity of carbon.[20] It suggests that the carbon phase prevents the growth of nanocrystals and improves the thermal stability of the mesostructure. Stucky and co-workers reported that mesoporous TiO_2 with highly crystallized structure can be stabilized by the amorphous carbon, which resulted from careful coking of the surfactant template.[4] Recently, TiO_2 nanoparticles coated with three-dimensionally ordered macroporous (3DOM, ~400 nm)[21] TiO_2−carbon composites[22] and TiO_2−graphitized-carbon composites[23] have been prepared using a colloidal templating approach. However, the carbon components in these composites are not homogenously dispersed, and the microporosity of carbon is sacrificed. Furthermore, the high carbon content in these composites also results in a reduction of the photocatalysis activity.

Herein, we demonstrate an organic−inorganic−amphiphilic coassembly approach to fabricate ordered mesoporous carbon−titania nanocomposites by using resols as an organic precursor, $TiCl_4$ as an inorganic precursor, and amphiphilic triblock copolymer F127 as a template. The TiO_2 nanocrystals are embedded in the pore walls and the mesostructured bricked-mortar frameworks are formed after calcination. The carbon−TiO_2 nanocomposites exhibit highly ordered two-dimensional (2D) hexagonal mesostructure and high thermal stability up to 700 °C. The nanocomposites have high surface area (465 $m^2\ g^{-1}$) and large pore size (~4.1 nm). The texture properties and compositions of the nanocomposites can be controlled by simply adjusting the initial mass ratios of $TiCl_4$ to resol. The carbon− titania nanocomposites also exhibit excellent photocatalytic activity in the decomposition of Rhodamine B (RhB) in aqueous suspensions.

Experimental Section

Chemicals. Amphiphilic poly(ethylene oxide)-*b*-poly(propylene oxide)-*b*-poly(ethylene oxide) triblock copolymer Pluronic F127 (M_w = 12600, $EO_{106}PO_{70}EO_{106}$) was purchased from Acros Corp. $TiCl_4$, phenol, formalin solution (37 wt%), NaOH, HCl, ethanol, and P25 were purchased from Shanghai Chemical Corp. All chemicals were used as received without any further purification. Millipore water was used in all experiments.

Synthesis of Ordered Mesoporous Carbon−Titania Nanocomposites. The carbon-titania nanocomposites were synthesized via the evaporation-induced triconstituent co-assembly followed by the in situ crystallization technology. First, a stock $TiCl_4$ solution (20 wt%) was prepared by dropping $TiCl_4$ into the mixture of ethanol and deionized water (7:1 EtOH:H_2O in mass ratio) at 0 °C under vigorous stirring for 30 min. In parallel, 1.5 g of triblock copolymer F127 was dissolved in 10.0 g of ethanol with 1.0 g of deionized water. Then, 7.0 g of $TiCl_4$ solution (20 wt%) was slowly added with stirring for 1 h at room temperature. The resol precursor (M_w < 500) used as a carbon precursor was prepared according to the previously reported method.[24] As soon as 1.5 g of 20 wt% resols ethanolic solution was added, the solution rapidly became nacarat and was stirred for additional 10 min. The homogeneous multicomponent mixture was transferred into dishes to evaporate ethanol at 30–40 °C for 24 h in an oven. After being dried, the membranes were heated at 100 °C for 24 h to increase the framework polymerization and stabilize the mesophase. The as-made products, orange and transparent membranes, were scraped from the dishes and ground into fine powders. Calcination was carried out in a tubular furnace at 450 °C for 2 h and 600 and 700 °C for 1 h under N_2 with a rate of 1 °C/min to remove the amphiphilic triblock copolymer templates and obtain mesoporous carbon−titania nanocomposites, denoted as 30C-70TiO_2-*x*, where *x* represents the heat-treatment temperature. The nanocomposites with different compositions in a wide range from 20 to 80 wt% TiO_2 were prepared according to the similar procedure by varying the mass ratios of resol to $TiCl_4$. The final products were assigned to *y*C-(100-y)TiO_2-600, where *y* represents the weight percentage of carbon content in the nanocomposites. Mesoporous pure TiO_2 as a reference was prepared according to the previous report.[10]

Characterization. The small-angle X-ray scattering (SAXS) measurements were taken on a Nanostar U small-angle X-ray scattering system (Bruker, Germany) using Cu Kα radiation (40 kV, 35 mA). The *d*-spacing values were calculated by the formula $d = 2\pi/q$ and the unit-cell parameters were calculated from the formula $a_0 = 2d_{10}/\sqrt{3}$. X-ray diffraction (XRD) patterns were recorded on a Bruker D4 X-ray diffractometer with Ni-filtered Cu Kα radiation (40 kV, 40 mA). Nitrogen sorption isotherms were measured at 77 K with a Micromeritics Tristar 3000 analyzer (USA). Before measurements, the samples were degassed in a vacuum at 200 °C for at least 6 h. The Brunauer−Emmett−Teller (BET) method was utilized to calculate the specific surface areas (S_{BET}) using adsorption data in a relative pressure range from 0.04 to 0.2. Using the Barrett−Joyner−Halenda (BJH) model, the pore volumes and pore size distributions were derived from the adsorption branches of the isotherms, and the total pore volumes (V_t) were estimated from the adsorbed amount at a relative pressure P/P_0 of 0.992. The micropore volumes (V_m) and micropore surface areas (S_m) were calculated from the *V*−*t* plot method using the equation $V_m/cm^3 = 0.001547I$, where *I* represents the *Y* intercepts in the *V*−*t* plots. The *t* values were calculated as a function of the relative pressure using the de Bore equation, t (Å) $=[13.99/(\log(p_0/p) + 0.0340)]^{1/2}$. Transmission electron microscopy (TEM) images were conduced on a JEOL 2011 microscope (Japan) operated at 200 kV. The sample for TEM measurements was suspended in ethanol and supported onto a holey carbon film on a Cu grid. Weight changes of the products were carried out on a Mettler Toledo TGA-SDTA851 analyzer (Switzerland) from 25 to 900 °C under nitrogen or air with a heating rate of 5 °C/min.

Photocatalytic Activity Measurement. The photodegradation of the xanthene dye Rhodamine B was carried out in a cylindrical flask (100 mL) as a photoreactor following the reported procedure.[22] Fifty milligrams of catalyst was magnetically stirred in a reactant solution, which contains 100 mL of Rhodamine B with an initial concentration of 5×10^{-5}M, in the dark for at least 30 min to reach the adsorption equilibrium of Rhodamine B with the catalyst. The solution was irradiated by a 125 W mercury lamp, which was placed in an inner irradiation cell made of quartz. The degradation rate was determined at different intervals by UV−Vis absorption (553 nm).

(20) Yu, Y.; Yu, J. C.; Chan, C. Y.; Che, Y. K.; Zhao, J. C.; Ding, L.; Ge, W. K.; Wong, P. K. *Appl. Catal., B* **2005**, *61*, 1.
(21) Wang, Z. Y.; Ergang, N. S.; Al-Daous, M. A.; Stein, A. *Chem. Mater.* **2005**, *17*, 6805.
(22) Zhang, D. Y.; Yang, D.; Zhang, H. J.; Lu, C. H.; Qi, L. M. *Chem. Mater.* **2006**, *18*, 3477.
(23) Lei, Z. B.; Xiao, Y.; Dang, L. Q.; You, W. S.; Hui, G. S.; Zhang, J. *Chem. Mater.* **2007**, *19*, 477.
(24) Meng, Y.; Gu, D.; Zhang, F. Q.; Shi, Y. F.; Yang, H. F.; Li, Z.; Yu, C. Z.; Tu, B.; Zhao, D. Y. *Angew. Chem., Int. Ed.* **2005**, *44*, 7053.

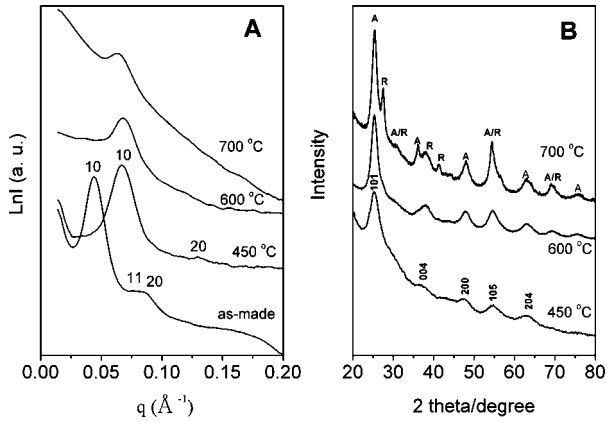

Figure 1. (A) SAXS patterns and (B) WAXRD patterns of as-made carbon−titania nanocomposite (30C-70TiO_2), and mesoporous carbon−titania nanocomposites calcined at 450, 600, and 700 °C.

Results and Discussion

Synthesis of Ordered Mesoporous Carbon−Titania Nanocomposites. We take the mesoporous nanocomposite 30C-70TiO_2-*x* with the carbon-compound content percentage of 30 wt% as an example, wherein *x* represents the heating temperature. The SAXS pattern (Figure 1A) of as-made 30C-70TiO_2 nanocomposite shows three resolved scattering peaks that can be indexed to 10, 11, and 20 reflections of 2D hexagonal symmetry (space group of *p*6*mm*),[25] suggesting a highly ordered mesostructure. After the calcination under an inert atmosphere (N_2) at 450 °C for 2 h, the SAXS pattern becomes poorly resolved, and two scattering peaks are observed, suggesting that the hexagonal mesostructure is retained. The degradation of the mesostructure is related to the elimination of the copolymer template[24,26] and the formation of nanocrystalline anatase in the frameworks during the thermal treatment process.[18] Furthermore, the 10 scattering peak shifts toward higher angle. The structural contraction ratio calculated from the difference in cell parameters (a_0) is 17.5% (Table 1). After the nanocomposites are further heated at 600 and 700 °C, the SAXS patterns become more poorly resolved and the intensities of the scattering peaks greatly decrease, suggesting that the mesostructure regularity further degrades. The calculated cell parameters are not significantly changed, indicating that the mesostructure is rigid and the shrinkage no longer occurs. Our results show that heating at 900 °C for 1 h leads to a complete collapse of the mesostructure.

TGA measurements (see the Supporting Information, Figure S1) show that the amphiphilic triblock copolymer F127 template can be removed after being heated under N_2 at 450 °C. The nanocomposite 30C-70TiO_2-600 shows 30 wt% weight loss in the range of 300–450 °C and 70 wt% weight residues. It suggests that the contents of carbon and titania are roughly 30 and 70 wt%, respectively, which is consistent with the synthesis compositions.

The wide-angle XRD (WAXRD) pattern of mesoporous nanocomposite 30C-70TiO_2-450 shows five broad diffraction peaks, indexed as 101, 004, 200, 105, and 204 reflections of anatase phase (Figure 1B), suggesting a formation of TiO_2 nanocrystals after heated at 450 °C. As the temperature increases, the diffractions especially for the 101 reflection at 2θ value of ~25.4° become narrow and intense, indicating a further growth and a size increase in TiO_2 nanocrystals. Additionally, a transformation from anatase to rutile phase occurs at 700 °C because rutile is the most stable phase, whereas the anatase is still the predominant phase. On the basis of the Scherrer formula, we estimate the average sizes of anatase nanocrystals treated at 450, 600, and 700 °C from the 101 reflections to be about 6.4, 9.1, and 11.4 nm, respectively (Table 1).

TEM images of the nanocomposite 30C-70TiO_2-450 show uniform (images A and B in Figure 2), well-ordered hexagonal channel arrays in large areas, indicating a highly ordered mesostructure.[25] Selected area electron diffraction (SAED) pattern (Figure 2A, inset) confirms that the anatase crystallites are indeed formed. After the nanocomposites are heated at 600 °C, the TEM image (Figure 2C) also shows well-defined hexagonal channels, suggesting that ordered mesostructure is retained, consistent with the result from the SAXS pattern. The SAED pattern (Figure 2C inset) becomes more resolved, suggesting a further growth of these TiO_2 nanocrystallites. Energy-dispersive X-ray (EDX) analysis of the ordered mesostructural domains for the nanocomposite 30C-70TiO_2-600 clearly shows the characteristic peaks of titanium, carbon, and oxygen, suggesting the coexistence of crystalline TiO_2 and carbon (Figure 2C inset). Also, the quantitative results of EDX clearly show that the weight percents of C and Ti are 30 and 39 wt%, respectively, which is consistent with the data (C, 30 wt% and Ti, 41.9 wt%) from TG analysis. It should be noted that a partly distorted mesostructure in some domains can be observed in the TEM images. High-resolution TEM (HRTEM) images (images D and E in Figure 2) clearly show that the anatase nanocrystallites are embedded in amorphous carbon matrixes, further suggesting the formation of the bricked-mortar frameworks. The HRTEM images (images D and E in Figure 2) also clearly show that some of the TiO_2 nanocrystals thrust into the mesochannels from the walls and block the pores. This may be one of reasons that the 11 and 20 scattering peaks become poorly resolved after the heat treatment. The sizes of the anatase nanocrystallite are measured from the HRTEM images to be 8.0 × 10.5 nm^2 for the nanocomposite 30C-70TiO_2-600, which is in agreement with the average crystallite size (~9.1 nm) calculated from the WAXRD patterns.

Figure 3 shows N_2 sorption isotherms and pore size distributions of the carbon−titania nanocomposites calcined at different temperatures. All of the nanocomposites exhibit representative type IV isotherms with H_2 type hysteresis loops.[25] It is related to imperfect cylinder channels, presumably driven by the growth of anatase nanocrystallites within the pore walls. Some of large TiO_2 nanocrystals can thrust into the channels and block the mesopores, which results in an ink-bottle pore and H_2 type hysteresis loop. A very sharp pore size distribution at a mean value of 4.1 nm was

(25) Zhao, D. Y.; Feng, J. L.; Huo, Q. S.; Melosh, N.; Fredrickson, G. H.; Chmelka, B. F.; Stucky, G. D. *Science* **1998**, *279*, 548.
(26) Liu, R. L.; Shi, Y. F.; Wan, Y.; Meng, Y.; Zhang, F. Q.; Gu, D.; Chen, Z. X.; Tu, B.; Zhao, D. Y. *J. Am. Chem. Soc.* **2006**, *128*, 11652.

Table 1. Physicochemical Properties of the Mesoporous Carbon–Titania Nanocomposites Prepared with Different Titania Contents and Heating Temperature[a]

sample name	a_0 (nm)	D_A (nm)	D (nm)	S_{BET} (m^2 g^{-1})	S_m (m^2 g^{-1})	V (cm^3 g^{-1})
80C−20TiO_2−600	10.5	3.0	3.6	465	268	0.26
50C−50TiO_2−600	10.6	6.7	3.9	295	140	0.24
30C−70TiO_2−450	10.6	6.4	4.1	191	41	0.19
30C−70TiO_2−600	10.6	9.1	3.6	276	97	0.18
30C−70TiO_2−700	10.6	11.4	3.2	346	101	0.20
20C−80TiO_2−600	11.0	11.0	4.0	209	48	0.16

[a] a_0, the unit-cell parameter, was calculated using the formula $a_0 = 2/d_{10}\sqrt{3}$. D_A, anatase nanocrystallite size, was calculated by Scherrer formula. S_{BET}, BET surface areas; S_m, micropore areas; D, pore size diameters; V, total pore volume.

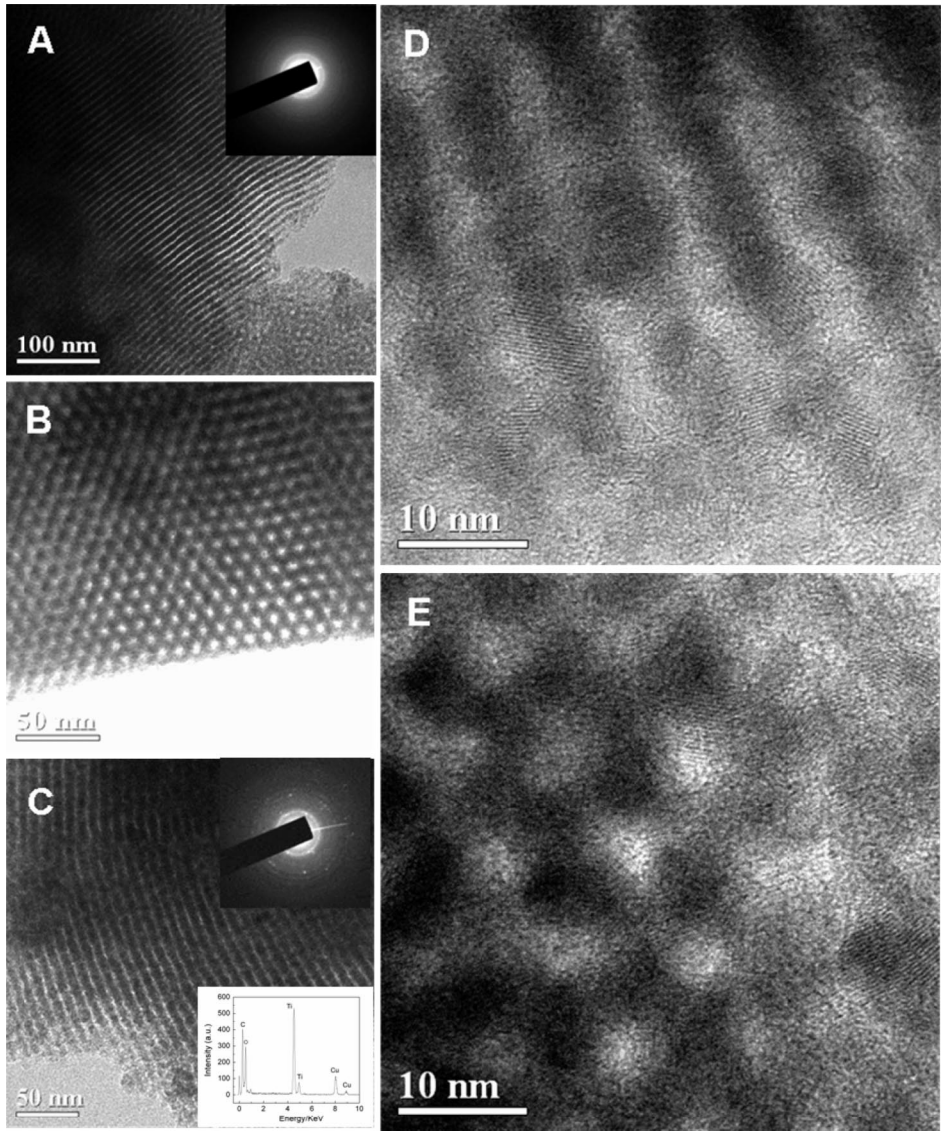

Figure 2. (A−C) TEM images, (D, E) HRTEM image of mesoporous carbon−titania nanocomposites (30C-70TiO_2-450 and 30C-70TiO_2-600) calcined at 450 (A, B) and 600 °C (C−E), viewed from the [110] (A, C, and D) and [001] (B, E) directions. Insets are the SAED patterns and EDX analysis taken at the same area.

calculated from the adsorption branch on the basis of BJH model. The mesoporous nanocomposite 30C-70TiO_2-450 has a surface area of 191 m^2 g^{-1} and pore volume of 0.19 cm^3 g^{-1}. As the temperature increases, the specific surface area and pore volume increase, whereas the mean pore size decreases (Table 1). The increase of BET surface area and pore volume may be attributed to the generation of a plenty of micropores in the frameworks, which mainly results from the glued carbon phase (Table 1 and the Supporting Information, Figure S2). The decrease in pore size reveals that the thickness of the pore walls increases from 6.5 to 7.4 nm. Compared with the size of the TiO_2 nanocrystallites from 6.4 to 11.4 nm (Table 1), the wall thickness is a little smaller, implying that some of TiO_2 nanocrystals could partially pierce even into the channel space, particularly evident in HRTEM images (panels D and E in Figure 2).

The TiO_2:carbon mass ratio of mesoporous carbon−titania nanocomposites can be varied in a wide range of 0.25–4

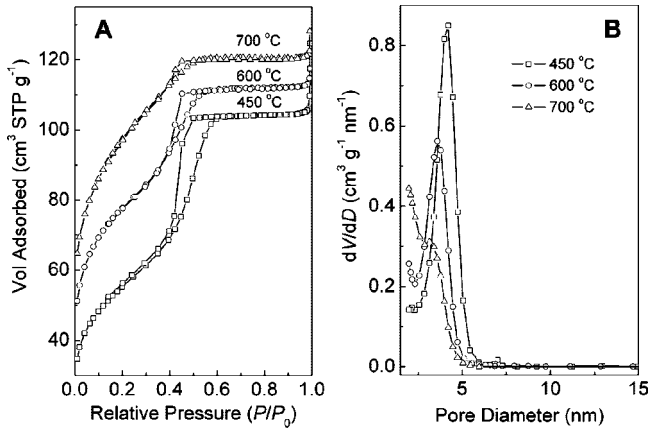

Figure 3. (A) N_2 sorption isotherms and (B) pore size distributions of the mesoporous nanocomposites 30C-70TiO_2 calcined at 450, 600, and 700 °C in N_2.

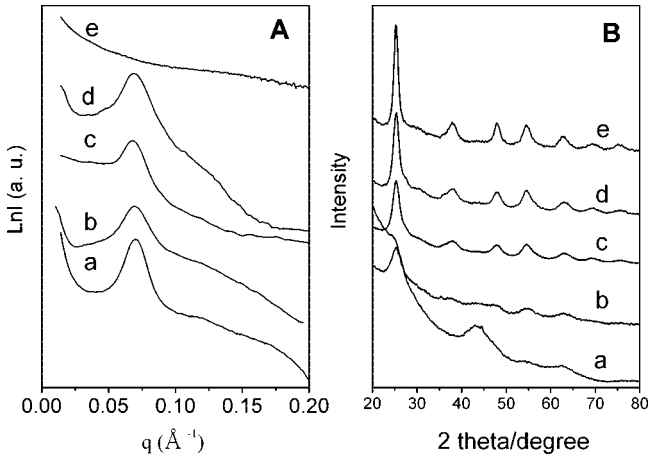

Figure 4. (A) SAXS patterns and (B) WAXRD patterns of the mesoporous carbon-titania nanocomposites with different titania percentage calcined at 600 °C in N_2. (a) 80C-20TiO_2-600, (b) 50C-50TiO_2-600, (c) 30C-70TiO_2-600, (d) 20C-80TiO_2-600, and (e) pure mesoporous TiO_2-600 prepared by using $TiCl_4$ as a precursor and triblock copolymer F127 as a template after calcination at 600 °C in N_2.

by varying the initial mass ratios of $TiCl_4$ to resols. The SAXS patterns of the nanocomposites with titania content (wt%) of 20, 50, 70, and 80 calcined at 600 °C in N_2 are shown in Figure 4A. All of the nanocomposites show one scattering peak with similar *d*-spacing of ~9.1 nm, suggesting that the ordered 2D hexagonal mesostructure is stable. TEM images (see the Supporting Information, Figure S3) further confirm that the nanocomposites even with high TiO_2 content (80 wt%) have well-ordered mesostructures. It is very clearly observed in the HRTEM image (see the Supporting Information, Figure S3C) that the nanocomposites composed of the randomly orientated anatase nanoparticles occupy the limited space within the channel walls. By contrast, no scattering peak can be observed in the SAXS pattern (pattern e in Figure 4A) for pure TiO_2 prepared by using amphiphilic triblock copolymer F127 as a template according to the same procedure as the reference,[10] indicating that its mesostructure is unstable and completely destroyed after calcination at 600 °C. It further provides evidence that the incorporation of the carbon can effectively improve the thermal stability of mesoporous titania.

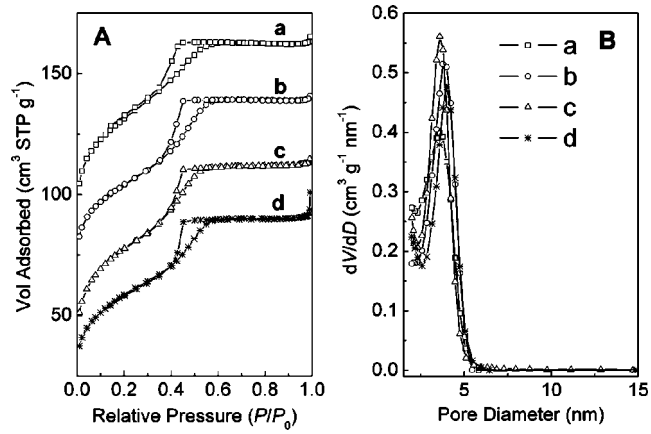

Figure 5. (A) N_2 sorption isotherms and (B) pore size distributions of the mesoporous carbon−titania nanocomposites with different carbon percentage calcined at 600 °C in N_2. (a) 80C-20TiO_2-600, (b) 50C-50TiO_2-600, (c) 30C-70TiO_2-600, and (d) 20C-80TiO_2-600. The isotherm of 50C-50TiO_2-600 is offset vertically by 35 $cm^3\ g^{-1}$ for clarity.

WAXRD patterns show characteristic diffractions for anatase (Figure 4B), suggesting the formation of TiO_2 nanocrystallites. When the titania content in the nanocomposite (80C-20TiO_2-600) is as low as 20 wt%, a broad diffraction peak at 2θ value of about 43° is observed, which corresponds to the 10 reflection of amorphous carbon. Another weak diffraction at 2θ value of about 24° is a superposition of the 002 and 101 reflections of carbon and anatase, respectively (pattern a Figure 4B). These results clearly suggest the coexistence of amorphous carbons and nanocrystalline TiO_2 in the mesostructural framework, although we could not exclude the amorphous TiO_2 in the nanocomposites. The WAXRD diffractions become narrow and intense with the increase in titania content, indicating an increase of nanocrystalline anatase size. The average crystallite size is calculated from XRD patterns to be in the range of 3.0–11.0 nm (Table 1).

N_2 sorption isotherms (Figure 5A) show that all of the nanocomposites exhibit similar type IV curves with distinct capillary condensation steps at a relative pressure of 0.45–0.55, suggesting a narrow mesopore size distribution at the mean value of about 3.6 nm, independent of titania content. Similar to that for 30C-70TiO_2-600 sample, H_2-type hysteresis loops are observed for these nanocomposites (Figure 5A), suggesting an ink-bottle mesopore. It is related to the block of the mesochannels by the large TiO_2 nanocrystals, which is in agreement with the HRTEM observation (see the Supporting Information, Figure S3C). On the other hand, as the TiO_2 content decreases, both BET surface areas and pore volumes greatly increase. It is mainly ascribed to the microporosity generated from the amorphous carbon phase in the nanocomposites.

Understanding the Mesostructured Nanocrystal-Glass Frameworks. Our results show that the successful synthesis of ordered mesoporous crystalline carbon−titania nanocomposites with high surface area and thermal stability in a wide range of TiO_2 contents (20–80 wt%) is mainly attributed to the preferred precursor of $TiCl_4$ and controlled EtOH solvent concentration. $TiCl_4$ can react with EtOH

to generate HCl acidities.[27,28] In the acidic condition, the protonation of phenol hydroxyl groups of the resols can prevent the transesterification reaction between titanate and polymer precursors. Highly ordered carbon−titania nanocomposites can be formed only in the presence of large amount of ethanol (EtOH:$TiCl_4$ mass ratio >5). It can be explained that the amount of ethanol determines the proton concentration in the initial solution and affects the hydrolysis of titanate and the subsequent condensation process. Our results also show that low relative humidity (<50%) facilitates the formation of the ordered mesostructure because of the sensitivity of $TiCl_4$ to H_2O. Similar to the carbon−silica nanocomposites,[26] we speculate that the formation of carbon−titania mesostructure undergoes an organic−inorganic−amphiphilic coassembly of the resols, titania oligomers, and amphiphilic triblock copolymer F127 during the solvent evaporation process. An interpenetrating hybrid network consisting of titania and cross-linked polymer resin is built during the thermopolymerization of resols at 100 °C inside the mesostructure framework. Unlike silica, TiO_2 phase easily nucleates and grows into nanocrystals during the heating process, resulting in amorphous carbon-crystalline TiO_2 nanocomposites with bricked-mortar frameworks. The amorphous carbon acts as a glue linking with the TiO_2 nanocrystals, preserves the mesostructure, and stabilizes the average regularity. The interaction between TiO_2 nanocrystals and amorphous carbons occurs via bridged oxygen atoms. Covalent bonds Ti−O−C on the surface and/or the coordination between Ti and HO−C groups may make the amorphous carbon act as a glue linking with TiO_2 nanocrystals.[4,22] However, further growth of TiO_2 requires the aggregation of separated TiO_2 phases, resulting in a collapse of the mesostructure. The attempts to prepare pure TiO_2 and carbon phases with ordered mesostructures by removing the carbon via the calcination in air at 550 °C and etching the TiO_2 with HF solution failed. Only disordered mesostructures of carbons and crystalline TiO_2 were obtained.

Photocatalytic Properties. The photocatalytic activity of the carbon−titania nanocomposites obtained at different temperatures was examined by measuring the photodegradation of Rhodamine B in an aqueous suspension following the reported procedure.[22] Under irradiation for 180 min (Figure 6A), the degradation percentages of Rhodamine B with carbon−titania nanocomposites calcined at 450, 600, and 700 °C are 70, 83, and 89%, respectively. The photodegradation of Rhodamine B roughly follows the pseudo-first-order reaction (Figure 6B), consistent with the previous reported results.[22,23] The rate constants are calculated to be 6.6×10^{-3}, 9.7×10^{-3}, and 11.2×10^{-3} min^{-1} for Rhodamine B with carbon−titania nanocomposites obtained at 450, 600, and 700 °C, respectively. These results indicate that the nanocomposite calcined at 450 °C exhibits the lowest photocatalytic activity, whereas the nanocomposite 30C-70TiO_2-700 exhibits the highest photocatalytic activity. It may be interpreted in terms of a compromise from the crystallinity and the surface area. Although the mesostructural regularity of the carbon−titania nanocomposites decreases with the increase in temperature, large surface area, and highly crystalline anatase obtained at high-temperature contributes high adsorptive capacity, resulting in high photocatalytic activity. For the comparison, the photodegradation of Rhodamine B was performed in the presence of the commercial Degussa P25 TiO_2 as a reference sample under the same condition. The rate constant for the sample P25 is measured to be 4.7×10^{-2} min^{-1}, which is a little higher than that of the obtained C−TiO_2 nanocomposites calcined at different temperatures. This phenomenon has been observed in the previous report,[22] which may be due to the smaller domain size of the crystalline TiO_2 in the nanocomposites compared with that of the powdered P25 sample. However, these C−TiO_2 nanocomposites can be formed as membranes, which may be easy to handle and considered as promising candidates for useful photocatalysts.

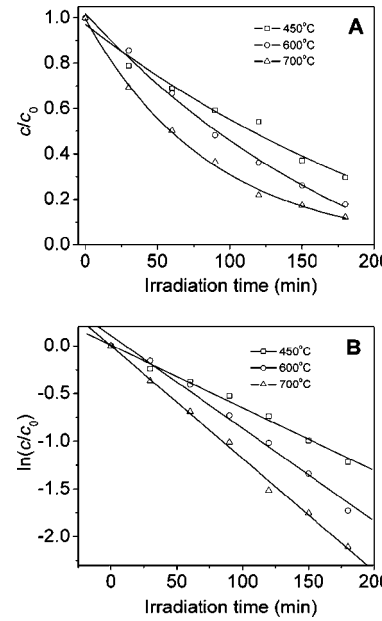

Figure 6. (A) Photocatalytic degradation of Rhodamine B monitored as the normalized concentration change versus irradiation time in the presence of mesoporous 30C-70TiO_2 nanocomposites calcined at 450, 600, and 700 °C in N_2. (B) Respective apparent first-order rate constant determined from the linear graph of $\ln(c/c_0)$ versus time.

Conclusions

We demonstrate a synthesis of highly ordered mesoporous carbon−titania nanocomposites with crystalline-glass frameworks via the organic−inorganic−amphiphilic co assembly followed by the in situ crystallization technology. The carbon−titania nanocomposites with controllable texture properties and composition can be obtained in a wide range from 20 to 80 wt% TiO_2 by adjusting the initial mass ratios. The nanocomposites possess ordered 2D hexagonal mesostructure, high surface area (up to 465 m^2 g^{-1}) and large uniform pore size (~4.1 nm). The presence of amorphous carbon phase acts as a

(27) Bradley, D. C. M. R. C.; Gaur, D. P. *Metal Alkoxides*; Academic Press: London, 1978.
(28) Crepaldi, E. L.; Soler-Illia, G.; Grosso, D.; Cagnol, F.; Ribot, F.; Sanchez, C. *J. Am. Chem. Soc.* **2003**, *125*, 9770.

glue linking with the TiO_2 nanocrystals and can improve the thermal stability of the mesostructure up to 700 °C. The carbon−titania nanocomposites show good photocatalytic activity for the photodegradation of Rhodamine B in an aqueous suspension, which may be attributed to the highly crystallized frameworks and high adsorptive capacity from the large surface areas. This approach may be applied to design many other ordered mesoporous crystalline carbon−M_xO_y nanocomposites with multifunctional properties.

Acknowledgment. This work was supported by NSF of China (20421303, 20521140450), State Key Basic Research Program of PRC (2006CB202502, 2006CB932302), Shanghai Science& Technology Committee (06DJ14006, 055207078, 05DZ22313), Shanghai Nanotech Promotion Center (0652nm024), Shanghai Education Committee (02SG01), and the Program for New Century Excellent Talents in University (Grant NCET-04-03). R. L. Liu acknowledges the support of Fudan Graduate Innovation Funds. We thank Dr. S. H. Xie for characterization assistance.

Supporting Information Available: TG analyses of as-made 30C-70TiO_2 nanocomposite in N_2 and 30C-70TiO_2-600 nanocomposite in air; EDX analysis of 30C-70TiO_2-600 nanocomposite, *t*-plot curves of mesoporous 30C-70TiO_2 nanocomposites calcined at 450, 600, and 700 °C in N_2; TEM images and HRTEM of 80C-20TiO_2-600 and 20C-80TiO_2-600 nanocomposites (PDF). This material is available free of charge via the Internet at http://pubs.acs.org.

CM071470W